摩擦学学报
TRIBOLOGY

不同厚度石墨烯表面的纳米摩擦各向异性研究

孔然，邹鲲

Nanofriction Anisotropy of Graphene Surface with Different Thickness

KONG Ran, ZOU Kun

在线阅读 View online: https://doi.org/10.16078/j.tribology.2021277

您可能感兴趣的其他文章

Articles you may be interested in

基于多尺寸微球探针石墨烯表面超低摩擦研究
Ultralow Friction Study on Graphene Based on Multi-Size Microsphere Probe
摩擦学学报. 2023, 43(8): 956 https://doi.org/10.16078/j.tribology.2022122

基于不同探针作用下石墨烯边界效应的摩擦调控
Friction Control of Graphene Boundary Effect Based on Different Probes
摩擦学学报. 2021, 41(5): 700 https://doi.org/10.16078/j.tribology.2020191

球形金属表面球磨制备石墨烯薄膜摩擦特性研究
Tribological Properties of Ball-Milling Graphene Films on Spherical Metal Surfaces
摩擦学学报. 2022, 42(3): 501 https://doi.org/10.16078/j.tribology.2021045

石墨烯负载铜纳米粒子微观摩擦行为的分子动力学模拟
Molecular Dynamics Simulation of Micro Friction Behavior of Graphene Loading Copper Nanoparticles
摩擦学学报. 2023, 43(4): 410 https://doi.org/10.16078/j.tribology.2021147

环氧树脂-水凝胶软硬复合表界面各向异性摩擦研究
Anisotropic Friction of Epoxy-Bydrogel Based Surfaces with Soft-Hard Combination
摩擦学学报. 2024, 44(3): 335 https://doi.org/10.16078/j.tribology.2023015

关注微信公众号，获得更多资讯信息

DOI: 10.16078/j.tribology.2021277

不同厚度石墨烯表面的纳米摩擦各向异性研究

孔 然, 邹 鲲*
(东华大学 机械工程学院，上海 201620)

摘 要: 考察石墨烯表面的纳米摩擦各向异性，研究厚度对其摩擦各向异性的影响. 采用原子力显微镜和高精度旋转台分析不同厚度石墨烯表面在不同方向的纳米摩擦特性. 结果表明：厚度为3.6 nm的石墨烯表面纳米摩擦表现出显著的各向异性但无周期性规律，原因是褶皱效应的产生增大了摩擦力. 厚度为7.5和14.7 nm的石墨烯表面纳米摩擦呈现180°和90°的周期性各向异性规律，归因于晶格结构取向和褶皱效应的共同作用. 厚度为24.5 nm的石墨烯主要受到晶格结构取向的作用，表面纳米摩擦呈现60°的周期性各向异性规律且沿扶手椅型晶格取向的摩擦力大于锯齿型晶格取向的摩擦力.

关键词: 石墨烯; 厚度; 摩擦各向异性; 原子力显微镜; 旋转台
中图分类号: TH117.3 **文献标志码:** A **文章编号:** 1004-0595(2023)03–0283–10

Nanofriction Anisotropy of Graphene Surface with Different Thickness

KONG Ran, ZOU Kun*

(*School of Mechanical Engineering, Donghua University, Shanghai 201620, China*)

Abstract: Graphene has a wide range of potential applications in micro/nano electromechanical systems (MEMS/NEMS) due to its excellent lubrication properties. In this paper, the nanofriction anisotropy of graphene surface with different thicknesses was investigated as the tip slides on graphene surface along with different directions by atomic force microscopy (AFM) and high-precision rotating table. The results showed that due to the extremely low out-of-plane stiffness of graphene with a thickness of 3.6 nm, a strong friction strengthening effect was generated in the stick-slip characteristic experiment after the tip sliding on the graphene surface. Then, graphene produced a great out-of-plane deformation and formed a puckering, which increased the contact area between the tip and graphene and thus increased the friction force. As a result, the nanofriction on the surface of graphene exhibited significant anisotropy with a large friction anisotropy ratio. The friction anisotropy ratio was the maximum friction in different angles divided by the minimum friction, and the great out-of-plane deformation leaded to the non-periodic friction of the tip along with all directions. The stiffness of graphene increased with the increase of the thickness leading to an enhanced effect of stick-slip characteristics experiment of small friction due to the weakened out-off-plane deformation, but the out-of-plane deformation did not disappear completely. The zigzag lattice spacing decreased and the armchair lattice spacing increased, which began to close two lattice structures of graphene itself, indicating that the lattice structure began to dominate friction anisotropy. Furthermore, the effect of out-of-plane deformation and lattice structure resulted in periodic anisotropy of 180° and 90° of nanofriction on the surface of graphene with 7.5 nm and 14.7 nm thickness. Due to the large out-of-plane stiffness of graphene with a thickness of 24.5 nm, the lateral force tended to be stable in the stick-slip characteristic experiment, and the friction strengthening effect disappeared, indicating the out-of-plane

Received 22 November 2021, revised 17 January 2022, accepted 18 January 2022, available online 25 January 2022.
*Corresponding author. E-mail: kouz@ dhu.edu.cn, Tel: + 86-13817889876.

deformation disappears. Moreover, the spacing between the zigzag lattice and the armchair lattice was almost consistent with the spacing of graphene itself. The results indicated that the frictional anisotropy was inhibited by the increased thickness of graphene and the frictional anisotropy dominated by the lattice structure orientation, resulting in a 60° periodic anisotropy of the surface nanofriction. Also, the friction along the armchair lattice orientation was greater than that along with the sawtooth lattice orientation. The coupling of structural anisotropy and thickness was the main factor of nanofriction anisotropy on the graphene surface. This work revealed the relationship between the different thicknesses of graphene and the anisotropy of surface nanofriction, which provided a theoretical basis for the design and application of graphene in micro and nanomechanical and electrical devices lubrication.

Key words: graphene; thickness; friction anisotropy; atomic force microscopy; rotating table

近年来，石墨烯由于非凡的电学[1]、热学[2]和光学[3]等特性[4]，在纳米电子器件中广泛应用. 二维材料的各向异性对其电学[5]、热学[6]和力学等性能有很大的影响[7-8]. 作为二维材料的石墨烯具有优异的摩擦学性能[9-11]，可作为理想的纳米润滑薄膜用于微/纳机电系统(MEMS/NEMS)活动构件的纳米间隙表面，减少构件表面间的摩擦磨损[12-15]. 因此，研究石墨烯的表面纳米摩擦特性与各向异性之间的关系可推动其在MEMS/NEMS的进一步发展.

通过探究石墨烯表面的摩擦各向异性可以研究石墨烯在特定方向上的超润滑特性[16]，其他二维材料也有着类似的研究[17-18]. 石墨烯的摩擦力具有层数依赖性，随层数的增加而减小，归因于层间局部接触刚度的增大降低了变形能[19]. 因此，厚度在原子级摩擦中起着至关重要的作用，其中摩擦各向异性比为不同角度下摩擦力的最大值除于最小值. 目前不同厚度石墨烯的表面纳米摩擦特性与各向异性之间关系的研究还比较缺乏. 鉴于此，本文中通过机械剥离将石墨烯转移至SiO_2/Si基底上，使用校准的原子力显微镜(AFM)和基于AFM的高精度旋转台研究不同厚度石墨烯摩擦力在不同旋转角度下的变化，分析不同厚度石墨烯的摩擦各向异性差异，提出不同厚度石墨烯的各向异性摩擦机理，进一步推动石墨烯的研究和应用.

1 试验部分

1.1 试验材料及制备

试验中使用的基底为P型掺杂的硅基底，表面覆盖了300 nm厚的SiO_2氧化层，为防止其表面含有污染物，需在乙醇溶液、丙酮溶液和去离子水中超声处理30 min，然后用氮气将其吹干. 石墨烯是通过从南京先锋纳米公司生产的天然石墨块体中机械剥离制备的. 机械剥离前将使用的SiO_2/Si基底加热1 min，温度为80 ℃左右，避免因为水汽的存在从而减小基底与石墨烯之间的黏附力. 待基底温度冷却后，进行石墨烯的转移，石墨烯转移的整个过程均在超净工作台中完成，防止空气中微尘的污染和水汽的干扰.

1.2 试验方法

试验中使用基于AFM的高精度旋转台为自主设计装置，每次旋转角度的精度小于0.05°，可以精确实现样品角度的旋转. 试验中使用的AFM型号为Asylum Research公司的MFP-3D型，使用的探针为Multi75Al-G型号的硅探针. 试验环境温度为24~28 ℃，相对湿度为55%~65% RH. 试验前先在光学显微镜下找到合适的样品位置并记录下来，再利用AFM的轻敲模式进行样品的形貌表征. 测摩擦力试验前，采用非接触法对探针进行法向和侧向的标定[20]，探针的侧向力常数为474 nN/V，测量摩擦的扫描范围为500 nm×500 nm，载荷为10 nN，扫描频率为1 Hz. 在摩擦扫描范围内选取中心的5 nm×5 nm区域内进行原子尺度的黏滑试验，载荷为10 nN. 当同一角度样品的形貌与摩擦试验完成后，利用旋转台进行不同角度样品的形貌表征与摩擦试验，以此研究石墨烯的表面纳米摩擦各向异性，其中摩擦试验区域取相同位置和大小.

2 结果与讨论

2.1 石墨烯的形貌表征

为探究不同厚度石墨烯的表面纳米摩擦各向异性，需选取不同厚度的石墨烯样品. 图1(a)所示为样品的光学图，红色和黑色方框处所对应的AFM照片如图1 (b)和(c)所示. 从图1 (b)和(c)插图可知白色横截线处的石墨烯的厚度分别为7.2和7.5 nm. 因此，图1(b)中石墨烯样品左右两侧的厚度分别为14.7和7.5 nm，其中黑色和黄色方框为试验区域. 同理，从图1(d)和(e)中插图可知白色横截线处的石墨烯的厚度分别为3.6和24.5 nm，其中黄色方框为试验区域. 由于石墨烯样品与基底贴合并非完全紧密，试验测得的石墨烯厚度可能会略大于理论值[21]. 为了保证石墨烯待测试验区域的平整性，对不同厚度石墨烯的试验区域进行粗糙度测量，

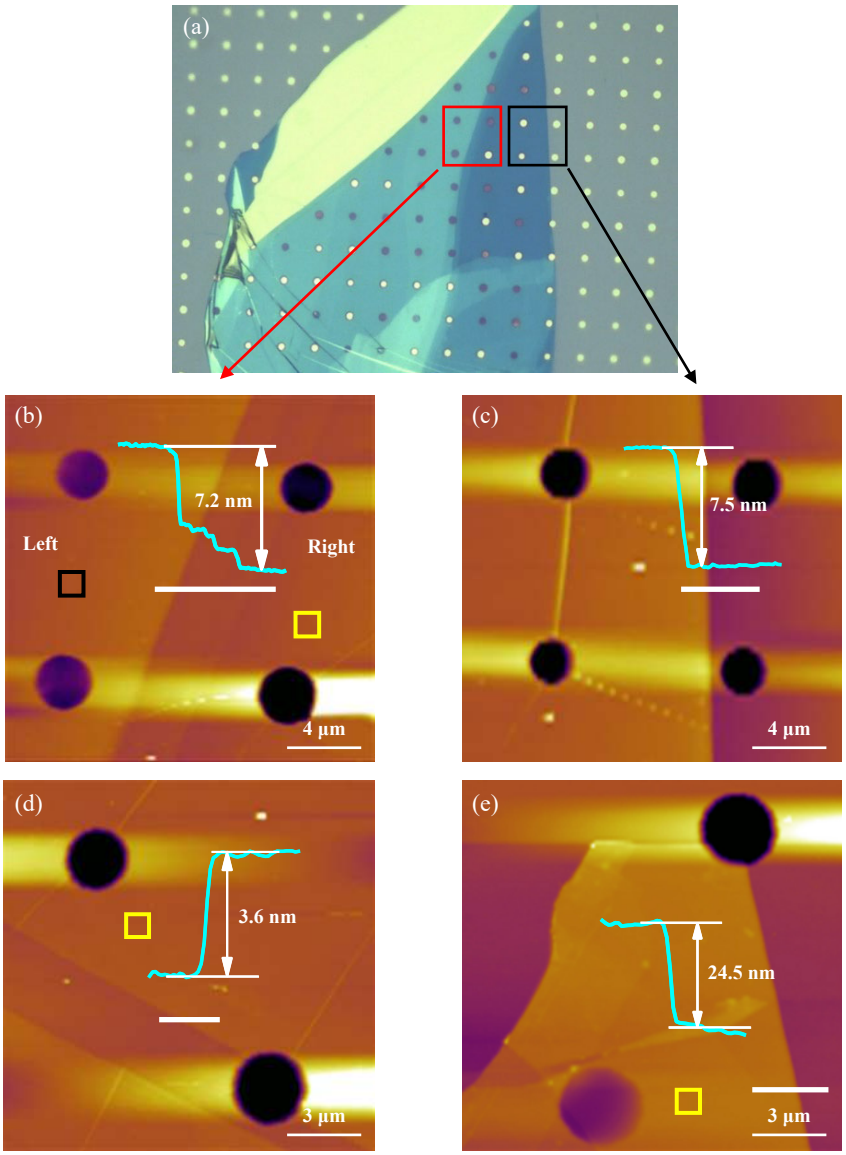

Fig. 1　(a) Optical image of graphene; (b~e) AFM micrographs of graphene (the illustration show the height profile of graphene)

图 1　(a)石墨烯的光学图; (b~e)石墨烯的AFM照片(插图为石墨烯的高度轮廓图)

粗糙度的均方根(RMS)维持在130 pm上下，符合摩擦试验的要求.

图2和图3分别所示为不同角度下厚度为3.6和24.5 nm石墨烯的AFM形照片，其中蓝色箭头表示原方向，黄色箭头代表旋转方向，红色旋转箭头代表旋转角度. 图4所示为厚度为7.5和14.7 nm石墨烯0°~330°的AFM照片，其中紫色虚线箭头表示原方向，蓝色实线箭头代表旋转方向，红色旋转箭头代表旋转角度. 上述所有角度的AFM照片都是通过石墨烯样品在高精度旋转台每次顺时针间隔旋转不同角度所测得的.

2.2　不同角度方向下石墨烯的摩擦力

在不同厚度石墨烯AFM照片中的试验区域进行不同角度下的摩擦试验，施加的固定载荷为10 nN，摩擦力的结果如图5和图6所示. 摩擦力的取值为线扫描的平均值，对不同角度下摩擦力数据进行汇总得到如图7所示的结果. 由图7(a)可知，石墨烯的厚度为3.6 nm时，摩擦力在各个方向表现出显著的差异，但无周期性规律. 然而，从图7(b~d)中摩擦力数据拟合的红色曲线可知，石墨烯厚度为7.5、14.7和24.5 nm的摩擦力随旋转角度的变化符合正弦函数规律，分别呈现180°、90°和60°的周期性各向异性规律.

2.3　摩擦各向异性的机理分析

由图8(a)可知，厚度较大石墨烯的摩擦各向异性比明显小于厚度较薄石墨烯的摩擦各向异性比. 原因是随着厚度的增加，石墨烯弯曲刚度增加，褶皱变形被抑制，导致相对摩擦力大小的差异减小. 为进一步

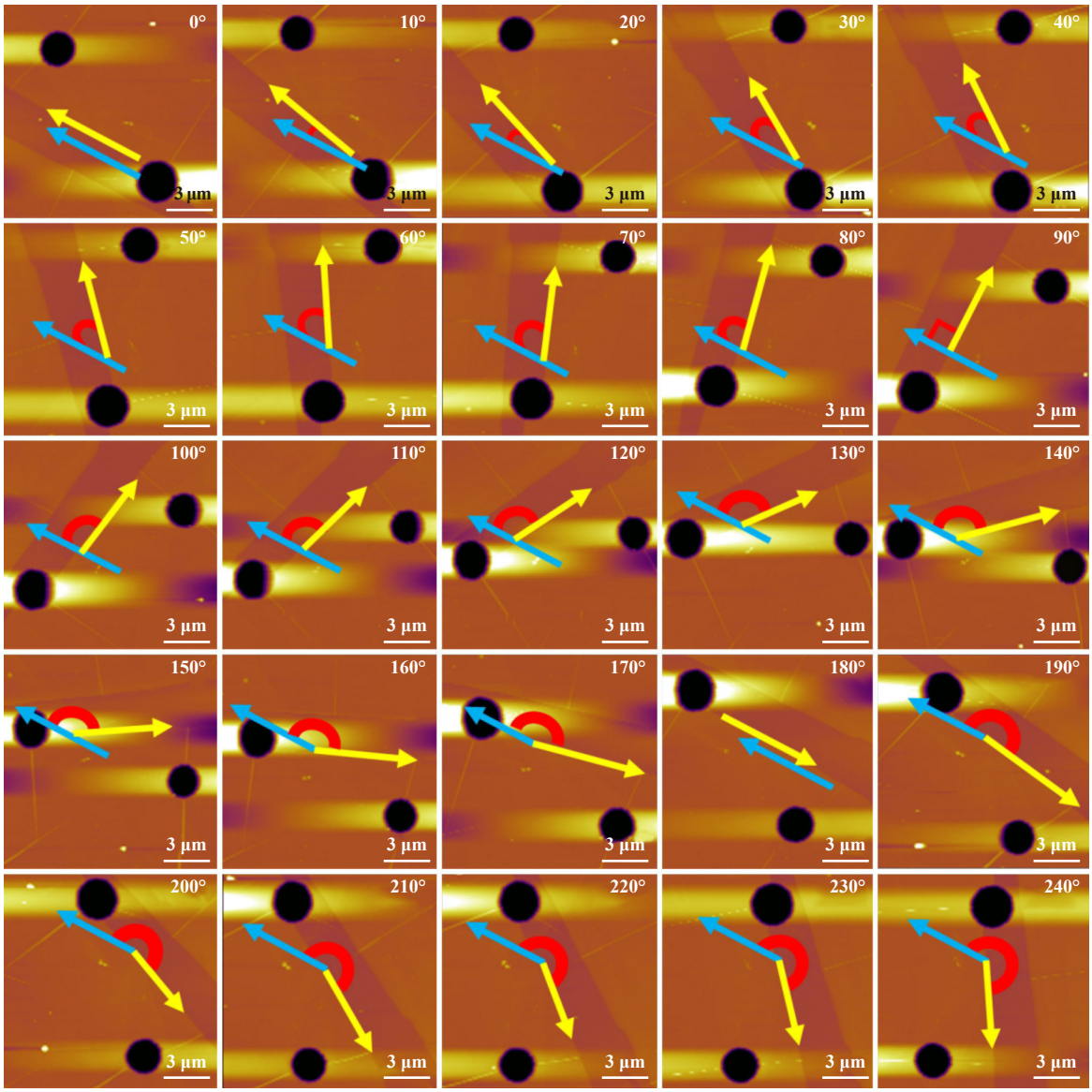

Fig. 2 AFM micrograph of graphene with a thickness of 3.6 nm rotated clockwise at 10° interval

图 2 石墨烯厚度为3.6 nm以10°间隔顺时针旋转的AFM照片

探究不同厚度石墨烯的表面纳米摩擦各向异性机理，对不同厚度石墨烯的不同晶格取向进行黏滑行为的特性研究，其中黏滑表现为侧向力曲线的锯齿状变化[22]. 图8(b~i)所示为AFM针尖在不同厚度石墨烯表面5 nm×5 nm扫描范围内测量的侧向力曲线，载荷为10 nN，黑色和红色曲线分别代表针尖在石墨烯的表面来回滑动过程中的侧向力大小，蓝色虚线和紫色垂直线分别代表与锯齿型和扶手椅型晶格周期相关的斜率和黏滑长度值. 其中摩擦力对应最小值的初始角度认为是石墨烯的锯齿型晶格取向，扶手椅型与锯齿型晶格取向角度相差30°. 图8(d~i)分别显示针尖尖端沿石墨烯表面的锯齿型和扶手椅型晶格取向扫描时的黏滑行为，其中石墨烯的晶格常数即锯齿型晶格间距约为0.246 nm，扶手椅型晶格间距与锯齿型晶格间距之比为1.731，大小约为$\sqrt{3}$. 结果显示，AFM针尖不连续的黏滑运动，类似于之前观察到的块状石墨和薄层石墨烯[23-26]. 由图8(b)和(c)可知，当石墨烯的厚度为3.6 nm时，不同旋转角度下的侧向力逐步上升出现摩擦增强效应，且晶格间距无明显大小的变化. 原因是薄层石墨烯较低的弯曲刚度导致更多的面外变形，沿锯齿型和扶手椅型晶格方向的巨大变形增强了摩擦各向异性. 由图8(d, e, g, h)可知，厚度为7.5和14.7 nm的石墨烯，扶手椅与锯齿型晶格取向的晶格间距比为1.498和1.573，小于$\sqrt{3}$，且蓝色虚线斜率较小，表现出弱摩擦强化特性，表明针尖在石墨烯表面滑动中受到了褶皱效应和晶格取向的共同作用. 由图8(f)和(i)可知，厚度

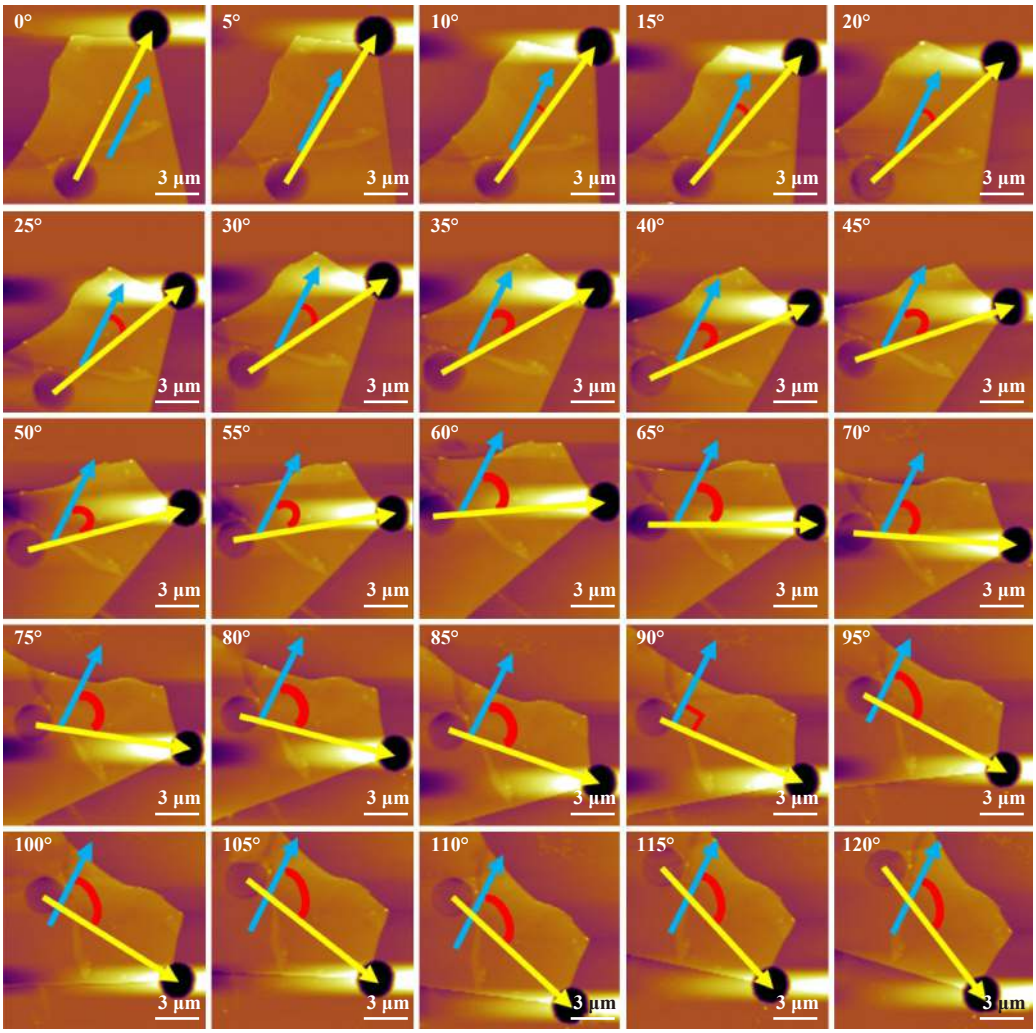

Fig. 3　AFM micrograph of graphene with a thickness of 24.5 nm rotated clockwise at 5° interval

图 3　厚度为24.5 nm的石墨烯以5°间隔顺时针旋转的AFM照片

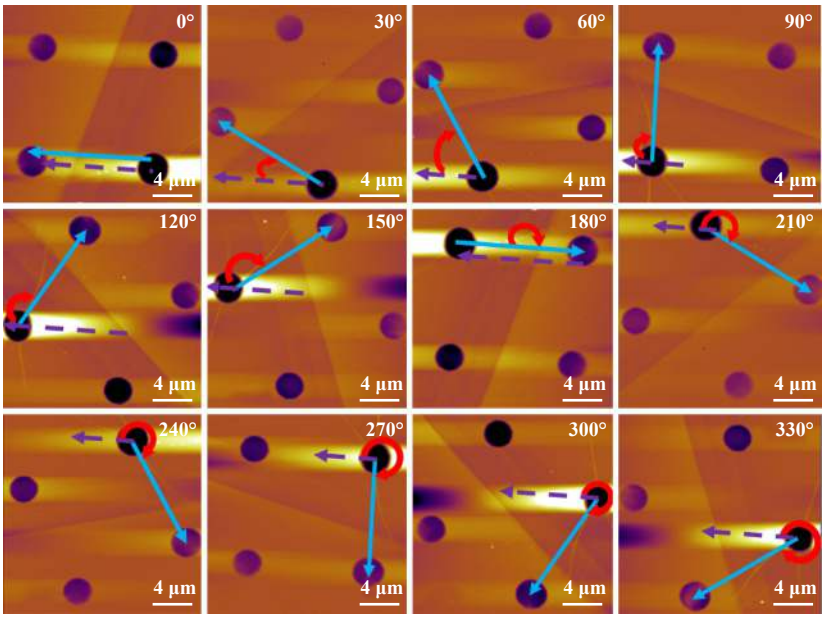

Fig. 4　AFM micrograph of graphene with thicknesses of 7.5 and 14.7 nm rotating clockwise at 30° intervals

图 4　厚度为7.5和14.7 nm的石墨烯以30°间隔顺时针旋转的AFM照片

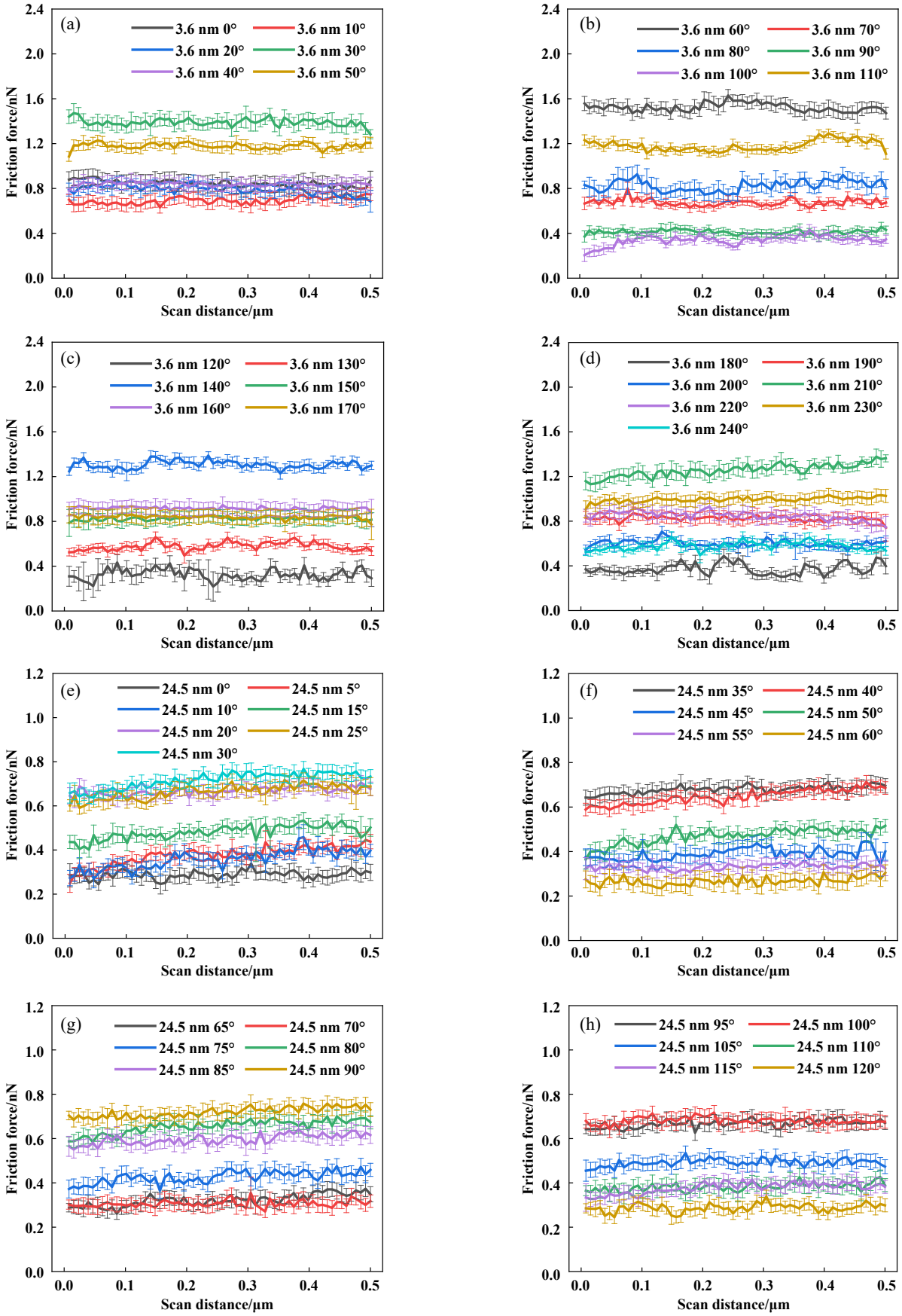

Fig. 5 Friction force of graphene with thickness of 3.6 and 24.5 nm at different rotation angles

图 5 厚度为3.6和24.5 nm的石墨烯在不同旋转角度下的摩擦力

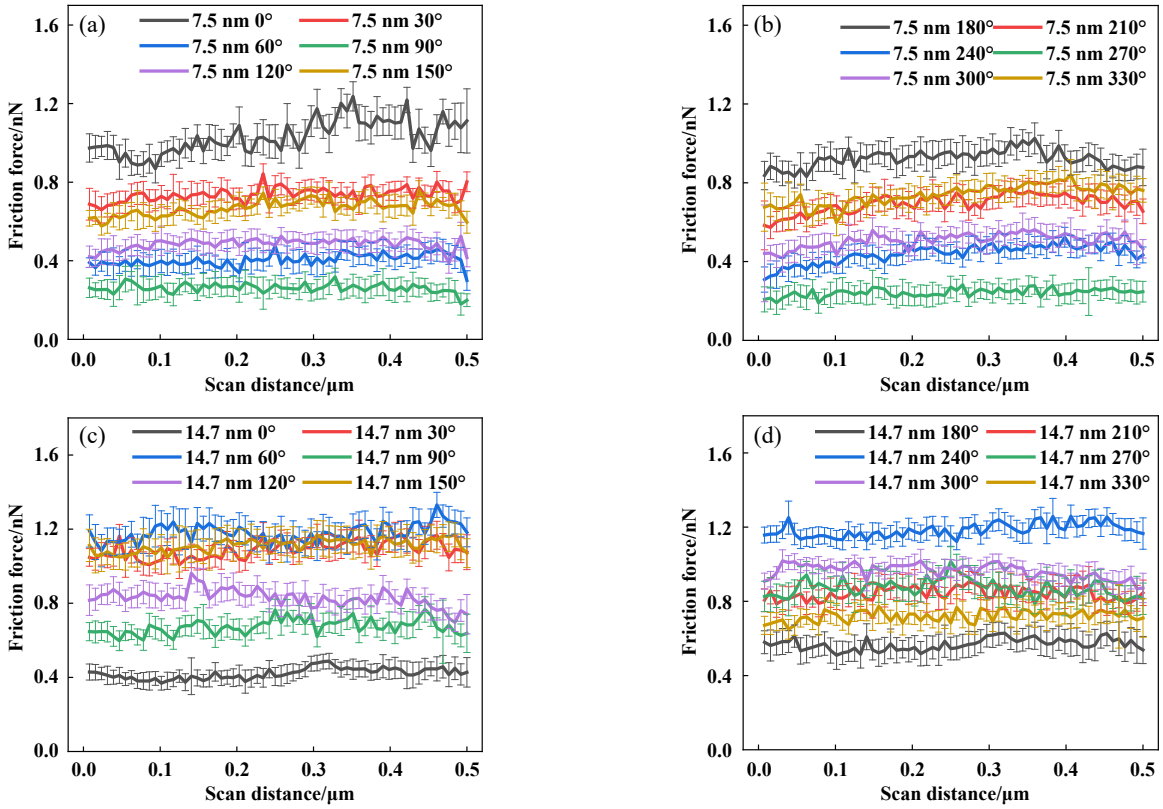

Fig. 6　Friction force of graphene with thickness of 7.5 and 14.7 nm at different rotation angles

图 6　厚度为7.5和14.7 nm石墨烯在不同旋转角度下的摩擦力

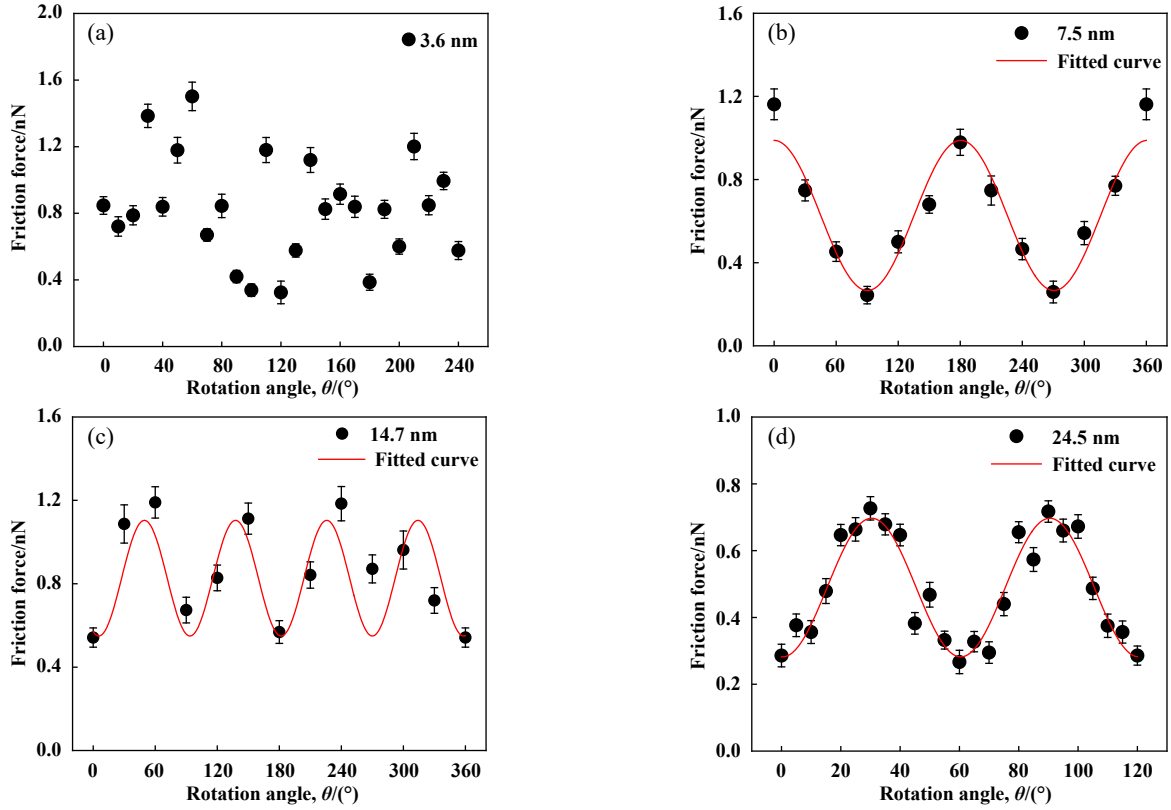

Fig. 7　Relationship between surface friction force and rotation angle of graphene with different thickness: (a) 3.6 nm; (b) 7.5 nm; (c) 14.7 nm; (d) 24.5 nm

图 7　不同厚度石墨烯的摩擦力与转角的关系: (a) 3.6 nm; (b) 7.5 nm; (c) 14.7 nm; (d) 24.5 nm

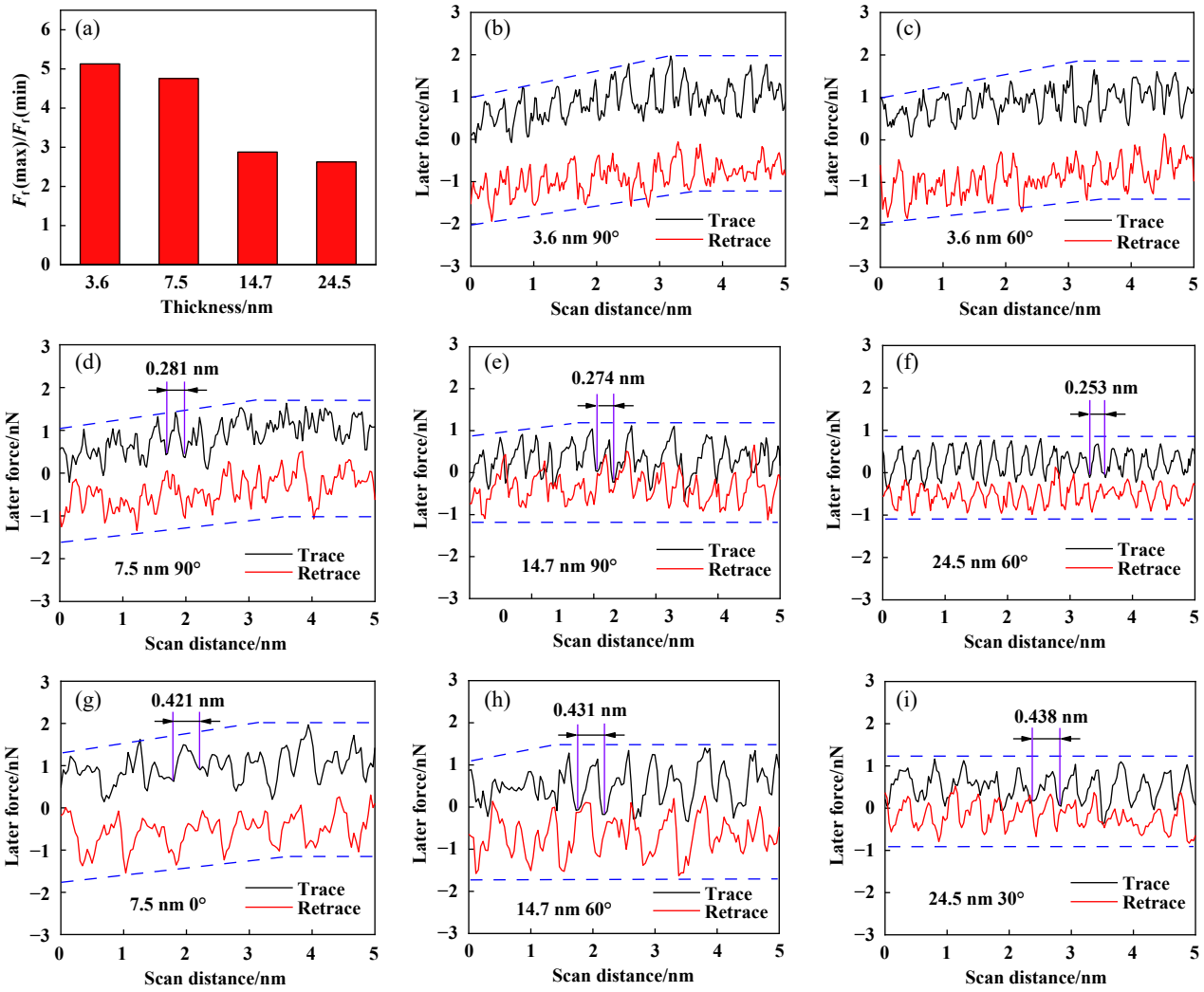

Fig. 8 (a) Anisotropy ratio of surface friction on graphene with different thickness; the lateral force curves of graphene with thicknesses of (b, c) 3.6 nm, (d, g) 7.5 nm, (e, h) 14.7 nm and (f, i) 24.5 nm

图 8 (a)不同厚度石墨烯的的摩擦各向异性比；厚度为(b, c) 3.6 nm、(d, g) 7.5 nm、(e, h) 14.7 nm 和 (f, i) 24.5 nm的石墨烯的侧向力曲线

为24.5 nm的石墨烯，扶手椅与锯齿型晶格取向的晶格间距比约为$\sqrt{3}$，且侧向力一直趋于平稳，表明针尖在石墨烯表面滑动中受晶格取向的主导作用，且沿锯齿型晶格取向的摩擦力小于扶手椅型晶格取向的摩擦力. 综上所述，当AFM纳米尺度的针尖在原子级厚度石墨烯表面进行初始侧向滑动时，石墨烯表面发生面外变形，并开始产生褶皱，侧向力开始逐渐增大. 当扫描过程中褶皱完全形成时，摩擦增强效果达到饱和，最终侧向力曲线趋于稳定的状态. 随着石墨烯的厚度增加，针尖扫描过程中摩擦增强特性逐渐削弱，原因是厚度越厚，其弯曲刚度越高，褶皱效应越弱[27]. 一旦褶皱效应消失，摩擦各向异性受晶格结构取向的作用，呈现60°周期性规律.

由上述试验可知，针尖在厚度为24.5 nm的石墨烯表面沿扶手椅型和锯齿型晶格取向滑动时没有褶皱变形的产生，晶格结构的周期性主导了其纳米摩擦呈现60°周期性的各向异性规律，如图9(a)所示. 图9(b)所示为石墨烯扶手椅型与锯齿型晶格方向的示意图，两种晶格之间的角度差值为30°. 图9(c)所示为针尖在厚度为3.6 nm石墨烯表面滑动的示意图，面外产生了严重的褶皱变形，导致不同晶格取向之间相对摩擦的差异增大，摩擦表现出显著的各向异性但无周期性规律. 图9(d)所示为厚层至薄层石墨烯表面的二维摩擦示意图，随着厚度越来越薄，针尖在石墨烯的摩擦滑动过程中的褶皱现象也越来越明显.

通过以上试验可知，石墨烯的晶格结构取向和褶皱变形是影响石墨烯表面纳米摩擦各向异性的重要因素. 随着石墨烯厚度的增加，褶皱变形被抑制直至

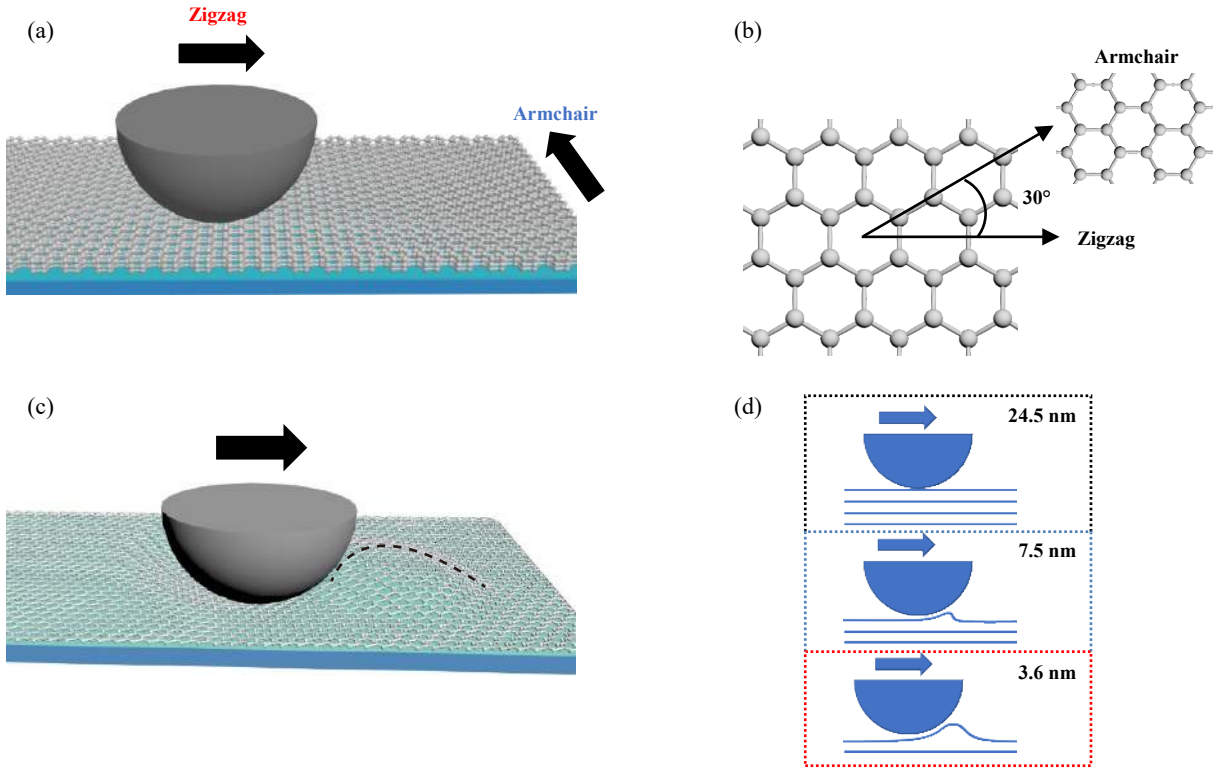

Fig. 9　(a) Schematic illustration of AFM tip sliding over graphene with a thickness of 24.5 nm along zigzag and armchair lattice orientation; (b) schematic diagram of graphene armchair and zigzag lattice orientation; (c) schematic illustration of AFM tip sliding over graphene with a thickness of 3.6 nm; (d) two-dimensional friction diagram of thick to thin layers of graphene

图 9　(a) AFM针尖在厚度为24.5 nm的石墨烯表面沿扶手椅型和锯齿型晶格方向滑动的示意图; (b)石墨烯扶手椅型和锯齿型晶格方向的示意图; (c) AFM针尖在厚度为3.6 nm的石墨烯表面滑动的示意图; (d)厚层到薄层石墨烯的二维摩擦示意图

消失，开始以褶皱作用为主导的摩擦各向异性会转变为以晶格结构取向为主导的摩擦各向异性，呈现不同角度的周期性规律，且沿锯齿型晶格取向的摩擦力小于扶手椅型晶格取向的摩擦力.

3　结论

a. 当石墨烯的厚度为3.6 nm，且针尖沿石墨烯表面扶手椅型与锯齿型晶格方向滑动时，有显著的摩擦增强效应. 原因是针尖在厚度较薄的石墨烯表面滑动时，主要受褶皱效应的影响，石墨烯的摩擦各向异性比大，摩擦力表现显著的各向异性，但无周期性规律.

b. 当石墨烯厚度为7.5和14.7 nm时，黏滑行为研究表明扶手椅型的晶格间距逐渐变大，锯齿型的晶格间距逐渐减小，即石墨烯的面外变形程度减小且摩擦增强效应被抑制. 原因是随厚度的增加，褶皱效应的作用被削弱，晶格结构取向开始起主导作用，两者的共同作用导致厚度为7.5和14.7 nm的石墨烯的摩擦分别呈现180°和90°周期的各向异性规律.

c. 当石墨烯的厚度为24.5 nm时，扶手椅与锯齿型晶格取向的晶格间距与石墨烯自身两晶格结构间距相同，无摩擦增强效应的产生. 原因是针尖在厚度很厚的石墨烯表面沿不同晶格取向滑动的过程中无褶皱变形的产生，摩擦各向异性受晶格结构取向的主导，导致石墨烯的摩擦呈现60°周期的各向异性规律.

参 考 文 献

[1] Schwierz F. Graphene transistors[J]. Nature Nanotechnology, 2010, 5(7): 487–496. doi: 10.1038/nnano.2010.89.

[2] Gupta A, Sakthivel T, Seal S. Recent development in 2D materials beyond graphene[J]. Progress in Materials Science, 2015, 73: 44–126. doi: 10.1016/j.pmatsci.2015.02.002.

[3] Wolverson D, Crampin S, Kazemi A S, et al. Raman spectra of monolayer, few-layer, and bulk $ReSe_2$: an anisotropic layered semiconductor[J]. ACS Nano, 2014, 8(11): 11154–11164. doi: 10.1021/nn5053926.

[4] Wang Yongxin, Hu Yiwen, Zhao Haichao, et al. Research progress of graphene as additives of water-based lubricants[J]. Materials Reports, 2021, 35(19): 19055–19061 (in Chinese) [王永欣, 胡艺纹, 赵海超, 等. 石墨烯基水润滑添加剂研究进展[J]. 材料导报, 2021, 35(19): 19055–19061]. doi: 10.11896/cldb.19050101.

[5] Xu Yang, Gao Haiyuan, Chen Huabin, et al. Electronic transport anisotropy of buckling graphene under uniaxial compressive strain:

Ab initio study[J]. Applied Physics Letters, 2012, 100(5): 052111. doi: 10.1063/1.3680092.

[6] Liu Xiangjun, Zhang Gang, Pei Qingxiang, et al. Phonon thermal conductivity of monolayer MoS_2 sheet and nanoribbons[J]. Applied Physics Letters, 2013, 103(13): 133113. doi: 10.1063/1.4823509.

[7] Torun E, Sahin H, Cahangirov S, et al. Anisotropic electronic, mechanical, and optical properties of monolayer WTe_2[J]. Journal of Applied Physics, 2016, 119(7): 074307. doi: 10.1063/1.4942162.

[8] Lei Zhouyue, Zhu Wencheng, Sun Shengtong, et al. MoS_2-based dual-responsive flexible anisotropic actuators[J]. Nanoscale, 2016, 8(44): 18800–18807. doi: 10.1039/c6nr07265h.

[9] Feng Xiaofeng, Kwon S, Park J Y, et al. Superlubric sliding of graphene nanoflakes on graphene[J]. ACS Nano, 2013, 7(2): 1718–1724. doi: 10.1021/nn305722d.

[10] Guo Chang, Zhang Xiaohui, Cai Jinming, et al. Research progress in application of graphene in nano-tribology[J]. Modern Chemical Industry, 2019, 39(11): 15–19,24 (in Chinese) [郭畅, 张晓慧, 蔡金明, 等. 石墨烯在纳米摩擦学中的研究进展[J]. 现代化工, 2019, 39(11): 15–19,24]. doi: 10.16606/j.cnki.issn0253-4320.2019.11.004.

[11] Chen Guangyan, Zhao Jun, He Yongyong, et al. Research progress on synthesis and structural control of graphene lubricant additives[J]. Tribology, 2021, 41(5): 758–772 (in Chinese) [陈广炎, 赵军, 何永勇, 等. 石墨烯润滑添加剂合成与结构调控[J]. 摩擦学学报, 2021, 41(5): 758–772]. doi: 10.16078/j.tribology.2020199.

[12] Chandross M, Lorenz C D, Grest G S, et al. Nanotribology of anti-friction coatings in MEMS[J]. JOM, 2005, 57(9): 55–61. doi: 10.1007/s11837-005-0117-y.

[13] Kim K S, Lee H J, Lee Changgu, et al. Chemical vapor deposition-grown graphene: the thinnest solid lubricant[J]. ACS Nano, 2011, 5(6): 5107–5114. doi: 10.1021/nn2011865.

[14] Peng Yitian, Wang Zhuoqiong, Zou Kun. Friction and wear properties of different types of graphene nanosheets as effective solid lubricants[J]. Langmuir:the ACS Journal of Surfaces and Colloids, 2015, 31(28): 7782–7791. doi: 10.1021/acs.langmuir.5b00422.

[15] Berman D, Erdemir A, Sumant A V. Graphene: a new emerging lubricant[J]. Materials Today, 2014, 17(1): 31–42. doi: 10.1016/j.mattod.2013.12.003.

[16] Dienwiebel M, Verhoeven G S, Pradeep N, et al. Superlubricity of graphite[J]. Physical Review Letters, 2004, 92(12): 126101. doi: 10.1103/PhysRevLett.92.126101.

[17] Liu Yanmin, Song Aisheng, Xu Zhi, et al. Interlayer friction and superlubricity in single-crystalline contact enabled by two-dimensional flake-wrapped atomic force microscope tips[J]. ACS Nano, 2018, 12(8): 7638–7646. doi: 10.1021/acsnano.7b09083.

[18] Claerbout V E P, Polcar T, Nicolini P. Superlubricity achieved for commensurate sliding: MoS_2 frictional anisotropy *in silico*[J]. Computational Materials Science, 2019, 163: 17–23. doi: 10.1016/j.commatsci.2019.03.019.

[19] Smolyanitsky A, Killgore J P, Tewary V K. Effect of elastic deformation on frictional properties of few-layer graphene[J]. Physical Review B, 2012, 85(3): 035412. doi: 10.1103/physrevb.85.035412.

[20] Wagner K, Cheng P, Vezenov D. Noncontact method for calibration of lateral forces in scanning force microscopy[J]. Langmuir, 2011, 27(8): 4635–4644. doi: 10.1021/la1046172.

[21] Nemes-Incze P, Osváth Z, Kamarás K, et al. Anomalies in thickness measurements of graphene and few layer graphite crystals by tapping mode atomic force microscopy[J]. Carbon, 2008, 46(11): 1435–1442. doi: 10.1016/j.carbon.2008.06.022.

[22] Kostoglou N, Polychronopoulou K, Rebholz C. Thermal and chemical stability of hexagonal boron nitride (h-BN) nanoplatelets[J]. Vacuum, 2015, 112: 42–45. doi: 10.1016/j.vacuum.2014.11.009.

[23] Schirmeisen A, Jansen L, Fuchs H. Tip-jump statistics of stick-slip friction[J]. Physical Review B, 2005, 71(24): 245403. doi: 10.1103/physrevb.71.245403.

[24] Verhoeven G S, Dienwiebel M, Frenken J W M. Model calculations of superlubricity of graphite[J]. Physical Review B, 2004, 70(16): 165418. doi: 10.1103/physrevb.70.165418.

[25] Bonelli F, Manini N, Cadelano E, et al. Atomistic simulations of the sliding friction of graphene flakes[J]. The European Physical Journal B, 2009, 70(4): 449–459. doi: 10.1140/epjb/e2009-00239-7.

[26] Xu Liang, Ma Tianbao, Hu Yuanzhong, et al. Vanishing stick-slip friction in few-layer graphenes: the thickness effect[J]. Nanotechnology, 2011, 22(28): 285708. doi: 10.1088/0957-4484/22/28/285708.

[27] Lee C, Li Q, Kalb W, et al. Frictional characteristics of atomically thin sheets[J]. Science, 2010, 328: 76–80. doi: 10.1126/science.1184167.